Проведено синтез і дослідження регуляторів дробового порядку, які для ряду технологічних процесів забезпечують найкращі показники якості перехідних процесів, зокрема для двигуна постійного струму з послідовним збудженням. Внаслідок залежності магнітного потоку від струму якоря та насичення магнітної системи якірний ланцюг двигуна характеризується як ланка з суттєвими нелинейними властивостями в статичних та динамічних режимах. Але з високою точністю його можна описати передавальною функцією дробового порядку. Завдяки відповідним дробовим інтегрально-диференційним регуляторам стає можливим забезпечити якість перехідних процесів значно кращу, ніж з класичними регуляторами.

Розглянуто стандартні методи синтезу коефіцієнтів регуляторів і встановлено, що подібні налаштування призводять до погіршення перехідних процесів через насичення регуляторів, викликаної обмеженням напруги джерела живлення. Отже, для замкнутого контуру з різними структурами дробових регуляторів було запропоновано використовувати генетичний алгоритм для визначення оптимальних значень коефіцієнтів регуляторів за критерієм найменшого часу першого узгодження і мінімального перерегулювання.

Експериментальні дослідження з різними структурами регуляторів проведено для налаштувань на модульний оптимум і дробовий порядок астатизму від 0.35 до 1.5. За отриманими результатами можна стверджувати, що найкращі показники забезпечують регулятори з астатизмом $1+\mu_{co}$, 1.5. Тоді перерегулювання фактично менше 2 %. Також показано, що при астатизмі $1+\mu_{co}$ забезпечується висока якість перехідних процесів і в зоні ненасиченої магнітної системи.

Результати дослідження можуть бути використані в першу чергу в системах замкнутого керування в двигунах постійного струму з послідовним збудженням, а також з об'єктами, в яких спостерігається степеневі закономірності

Ключові слова: дробове обчислення, регулятори з дробовим порядком диференціювання і інтегрування, двигун послідовного збудження

UDC 621.313.222:681.5.033.2, 621.316.7
DOI: 10.15587/1729-4061.2019.161352

SYNTHESIS AND IMPLEMENTATION OF FRACTIONAL-ORDER CONTROLLERS IN A CURRENT CURCUIT OF THE MOTOR WITH SERIES EXCITATION

V. Busher
Doctor of Technical Sciences, Professor*
E-mail: victor.v.bousher@gmail.com
L. Melnikova
PhD, Associate Professor*
E-mail: lubov.v.melnikova@gmail.com
V. Horoshko
Postgraduate student*
E-mail: vas.goroshko@gmail.com
*Department of Electromechanical Systems with Computer Control
Odesa National Polytechnic University
Shevchenka ave., 1, Odesa, Ukraine, 65044

1. Introduction

Development of the theory of fractals has sparked increased interest in the phenomena of self-similarity, characteristic of power laws, as well as the mathematical analysis of non-integer orders [1]. The latter is based on the systematic use of concepts on derivatives and integrals, whose orders are not integers, but could be fractional, irrational, and complex. Related to this is the invention by L. Euler of the continuation of factorial function $n!=1\cdot2\cdot...\cdot n$ in the domain of real and complex numbers, implemented by gamma function

$$\Gamma(v)=\int_0^{\infty}e^{-x}x^{v-1}\mathrm{d}x,\ \ \Gamma(n+1)=n!. \qquad (1)$$

Its application led to a breakthrough into the domain of non-integer number of degrees of differentiation and integration operators [2]. Owing to this, a family of differential equations is enriched. The presnece in the equations of a fractional derivative for time is interpreted as a reflection of the special property of the described process – memory, or, in the case of a stochastic process, a non-Markovian character.

The fractional calculus is considered to originate in the year of 1695, when Leibniz, in a letter to François L'Hôpital, discussed the differentiation of the non-integer order ½. More than 300 years have passed with many studies addressing this issue. The renewed interest in it has been evident over recent decades. That is primarily related to that the differential equations of fractional order often make it possible to describe physical processes with a greater accuracy than do the integer ones. Such a mathematical notation has been used in various fields, specifically acoustics, electronics, thermodynamics, and many others [3–7].

Theory of automatic control employs, in turn, fractional calculus as a mathematical apparatus to study the output coordinates in a series of systems with specific properties. For example, $PI^{\gamma}D^{\mu}$ controllers are used that make it possible to improve the quality of transient processes in comparison

with the classical integer PID controllers. That relates not only to that controllers also employ fractional calculus, but it also gives a certain freedom in the choice of a decimal degree for differential and integral components. Another advantage of such regulators is the possibility of increasing the reserve of stability compared to the integers.

When applying fractional-order regulators, such systems, relative to the control object, can be categorized in the following way:

– integer controller – integer control object;

– fractional-order controller – integral control object;

– integer controller – control object of fractional order;

– fractional-order regulator – control object of fractional order.

Fractional calculus can be used to describe electrical machines with adjustable magnetic flow, due to which the saturation of the magnetic system occurs. Paper [8] studied the influence of a magnetization curve on the characteristics of asynchronous electric machines; however, the apparatus of fractional integral-differential calculus was not applied.

In a DC motor with series excitation (DCMSE), as well as in generic engines, armature is connected in series with the excitation winding. Consequently, there develops a high starting torque at good indicators for weight and dimensions. Disadvantages include the complexity of implementing closed control systems, since DCMSE have nonlinear properties, predetermined by a magnetization curve and dependence of flow on armature current. However, this same property makes them an excellent study object using the apparatus of fractional calculus, thereby making it possible to compensate for the non-linear dependence and synthesize controllers that optimize the behavior of a closed system.

Given the wide scope of application of such machines in different fields of technology, it is a relevant task to improve the accuracy of control by employing new methods of analysis and synthesis.

2. Literature review and problem statement

A large body of research into control over DCMSE has been accumulated since 1970s. Thus, papers [9, 10] proposed controllers with changing, time-variable, parameters. Types of control methods vary from application of a nonlinear PI controller [11, 12] to fuzzy logic [13] and neural networks [14]. Such methods differ from conventional methods of synthesis of regulators for closed systems, which somewhat complicates the configuration process. Therefore, fractional-order regulators have been investigated recently. That makes it possible to take into consideration the non-linearity of control object, as well as to apply standard setting methods (for example, modular optimum). This relates to that the fractional-order transfer functions are similar to the integer ones, therefore, the methods used in the theory of linear continuous systems also apply to them.

Thus, paper [15] employed a $PI^{\gamma}D^{\mu}$-controller for speed of engine with independent excitation. To implement the fractional component, the authors used a higher-order transfer function approximation. Inner current circuit was not considered. Article [16] reported a PI^{γ}-controller of speed and a PD^{μ}-controller of position. Paper [17] used a sliding mode servo system and a fractional derivative in the speed circuit. Work [18] shows the possibilities to optimize controllers with a parametrically uncertain structure. Despite the different methods for calculating coefficients, it was shown that such controllers can help obtain transient processes with better parameters than when implementing the integer differentiation and integration. However, there are still unresolved issues related to the optimization of a current circuit and the settings for a fractional order of astatism greater than unity, which ensure a greater dynamic accuracy of the system. The reason for this is the difficulty of calculating these components based on discrete definitions by Riemann-Liouville, Grunwald-Letnikov, Caputo, Weyl, Erdelyi-Kober, etc. [19]. In any case, calculations come down to the requirement for storing maximally possible arrays of data and coefficients and computing the sums of their pairwise products. Accordingly, costs of CPU time grow significantly and memory volume requirements increase.

Thus, for example, fractional differentiation in the form of Grunwald-Letnikov requires that calculation should be performed according to formula:

$$ {}_aD_t^{\gamma} f(t) = \lim_{h\to 0} h^{-\gamma} \sum_{j=0}^{\left[\frac{t-a}{h}\right]} (-1)^j \binom{\gamma}{j} f(t-jh), \quad (2) $$

where a, t are the calculation bounds, $\gamma \epsilon R$ is the fractional exponent.

For fractional integration, the form of Grunwald-Letnikov is as follows:

$$ {}_aI_t^{\gamma} f(t) = \frac{1}{(\gamma)} \int_a^t \frac{f(\tau)}{(t-\tau)^{1-\gamma}} d\tau, \quad (3) $$

where Γ is the gamma function.

Attempts to resolve such a problem have led to constructing several groups of methods. Some of these methods assume that links that include derivatives and integrals of fractional order have a constant phase-frequency characteristic $\pm\frac{\pi}{2}\gamma$. Therefore, over a certain frequency range, it is acceptable to approximate with the link of higher integer orders from the left- and right-hand sides of the differential equation, which ensures an approximately constant phase shift [20, 21]. Other methods approximate dependences of coefficients on an array number, which reduces the time of computation [22]. Applying these methods makes it possible to employ fractional-order regulators in high-speed systems, specifically, in a current circuit of electric machines.

A DCMSE magnetization curve is close enough to a power dependence. It can therefore be assumed that $PI^{\gamma}D^{\mu}$-controllers could prove to be effective at optimizing the characteristics of a current circuit. The results obtained could be applied to other systems with similar properties as well.

3. The aim and objectives of the study

The aim of this study is to synthesize DCMSE current controllers with a fractional order of integration and differentiation in order to ensure the highest performance speed at small overshoot under the predefined order of astatism.

To accomplish the aim, the following tasks have been set:

– to study experimentally a motor with series excitation and to find an adequate mathematical model of a current circuit based on fractional-differential equations;

– to synthesize controllers to ensure several setting options with the required quality of transient processes and different astatism order, including under conditions for power supply voltage limitation;

– to undertake a study at different levels of job surges in order to assess the degree of self-similarity of the system with fractional integral-differentiating regulators.

4. Studying the transient current processes in a motor with series excitation

The object of our study was an Italian engine, made by CESET, the series MCA 38/64-148/AD8 with a rated frequency of ω_n=12,800 rpm, current I_n=1.6 A, and power P_n=370 W. Current was measured by the analog sensor ACS712, based on the Hall effect. The 12-bit analog-to-digital conversion and data entry were performed by the software recorded on the debug board STM32F4DISCOVERY clocked at 168 MHz. The engine was supplied voltage from the power supply unit Moeller SN3-100-BV8 24 V: it was regulated by using a pulse-width four-quadrant inverter.

Mathematical notation of the electromechanical energy conversion at DCMSE (excluding eddy currents) takes the following form [23]:

$$\begin{cases} u_a(t) = R_{a\Sigma}\cdot i_a(t) + L_{a\Sigma}\cdot\dfrac{di_a(t)}{dt} + k\cdot\Phi(t)\cdot\omega(t) + w_f\cdot\dfrac{d\Phi(t)}{dt}, \\ M(t) = k\cdot\Phi(t)\cdot i_a(t), \\ M(t) - M_s(t) = J_\Sigma\dfrac{\omega(t)}{dt}, \end{cases} \quad (4)$$

where $R_{a\Sigma}=R_a+R_{ap}+R_f$ is the total resistance of armature circuit; w_f is the number of turns of the excitation winding; $L_{a\Sigma}$ is the inductance of the motor armature circuit scattering; $\Phi(t)$ is the magnetic flux of the motor; k is the structural factor; J_Σ is the total moment of inertia on motor shaft; $\omega(t)$ is the motor's angular velocity; $M(t)$ is the torque generated by motor; $M_s(t)$ is the static torque on shaft.

Inductance scattering $L_{a\Sigma}$ is much less than the inductance of excitation winding $L_{f\Sigma}$. However, one should not neglect it in the study of dynamic processes because at $L_{a\Sigma}$=0 the jump-like changes in voltage applied to the motor, according to (4), must cause instantaneous changes in the motor's current, which is impossible.

It is important to note that equations (4) contain not only a non-linear dependence, but also its derivative, which does not make it possible to linearize the system by including the inverse nonlinear function in the closed circuit.

Fig. 1 shows a schematic diagram of the motor based on equations (4).

We shall highlight a current circuit excluding the motor's EMF (it is dashed in Fig. 1).

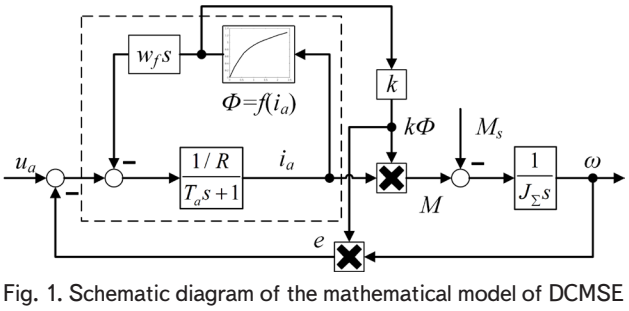

Fig. 1. Schematic diagram of the mathematical model of DCMSE

If the motor current is relatively small, the magnetization curve in this region is almost linear, hence the current circuit can be described by an inertial link of the first order. We shall determine its time constant based on the transient process at a voltage of 10 V at which there is no saturation in the excitation winding (Fig. 2). The result from data processing is the derived time constant – T_a=0.0267 s.

Build a closed system to control this object.

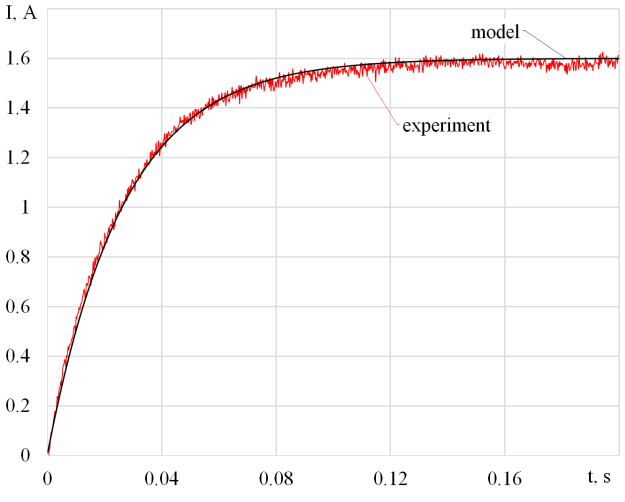

Fig. 2. Experimental and estimated diagrams of transient processes in the armature circuit at a voltage of 10 V

Determine a transfer function of the current controller $W_{cr}(s)$ to ensure setting the closed circuit to modular optimum:

$$W_{op.c}(s) = W_{cr}(s)\frac{k_{conv}}{(T_{\mu c}s+1)}\frac{1/R_a}{(T_a s+1)}k_{cs} = \frac{1}{2T_{\mu c}s(T_{\mu c}s+1)}, \quad (5)$$

where

$$W_{cr}(s) = \frac{1}{2T_{\mu c}s(T_{\mu c}s+1)}\cdot\frac{(T_{\mu c}s+1)(T_a s+1)R_a}{k_{conv}k_{cs}}. \quad (6)$$

We obtain upon transforms

$$W_{cr}(s) = K_1 + K_2 s^{-1}, \quad (7)$$

where

$$K_1 = \frac{T_a R_a}{2T_{\mu c}k_{comv}k_{cs}}, \quad K_2 = \frac{R_a}{2T_{\mu c}k_{comv}k_{cs}}. \quad (8)$$

When setting the current below the rated (1.6 A), the transient processes correspond to the theoretical ones. However, at big settings, there are significant differences (Fig. 3).

In order to synthesize the optimized system, we shall identify a control object while supplying the maximally permissible voltage by a surge (Fig. 4).

In order to mathematically describe the transient process, we considered the following transfer functions of control object:

$$W_{co1} = \frac{K}{a_0 s^{\mu}+1}, \quad (9)$$

$$W_{co2} = \frac{K}{a_1 s + a_0 s^{\mu}+1}, \quad (10)$$

$$W_{co3}=\frac{K}{a_1 s^{1+\mu}+a_0 s^{\mu}+1}. \quad (11)$$

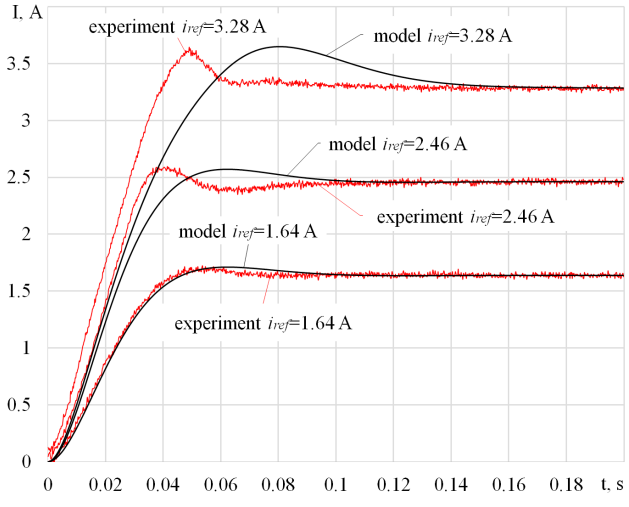

Fig. 3. Diagrams of transient processes for the model and the experiment with a PI-controller

To identify the unknown coefficients in (9) to (11), we used a genetic algorithm, in which the tournament method was chosen during selection; new individuals inherited the genes of parents through uniform crossbreeding, the likelihood of mutation in a chromosome is 20 % [24]. Estimate for the fitness of an individual was the standard error *F*. Results of identification of transfer functions are summarized in Table 1.

Table 1

Results of identification of transfer functions

Parameter	Transfer function of control object		
	W_{co1}	W_{co2}	W_{co3}
μ	1.14034	0.63744	0.35327
a_0	0.014138	0.04951	0.12709
a_1	0	0.02439	0.006193
K	0.16228	0.17048	0.19278
F	0.0079	0.0163	0.0039

Experimental and estimation diagrams are compared in Fig. 4.

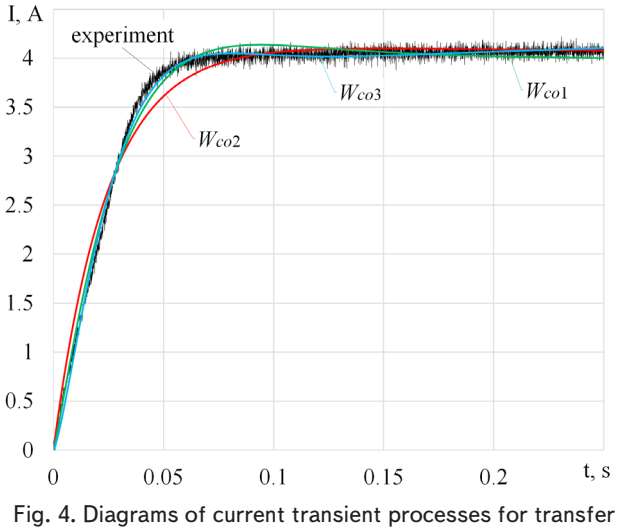

Fig. 4. Diagrams of current transient processes for transfer functions W_{co1}, W_{co2}, W_{co3} and for experimental data

It is obvious that the best transfer function is W_{co3}, which will be further used in the synthesis of controllers.

5. Synthesis of closed current circuit with optimal transient characteristics

We shall analyze the closed system to control DCMSE current at various settings.

Schematic diagram of a closed current control system is shown in Fig. 5. Denotations: u_{ref}, u_{cs}, Δu_r, u_a, i_a are the current and feedback setting signals, the error between them, the armature voltage and current, respectively. In addition: $W_{cr}(s)$, $W_{conv}(s)=\frac{k_{conv}}{T_{\mu c}s+1}$, $W_{cs}(s)=k_{cs}$, $W_{co}(s)$ are the transfer functions of current controller, converter, current sensor and control object, respectively.

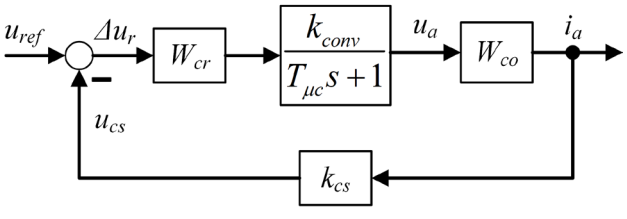

Fig. 5. Schematic diagram of the current control system

Determine the transfer function of current controller $W_{cr}(s)$ based on the settings on modular optimum, taking into consideration a magnetization curve:

$$W_{op.c}(s)=\frac{1}{2T_{\mu c}s\left(T_{\mu c}s+1\right)}=$$
$$=W_{cr}(s)\frac{k_{conv}}{\left(T_{\mu c}s+1\right)}\frac{K}{\left(a_1 s^{1+\mu}+a_0 s^{\mu}+1\right)}k_{cs}, \quad (12)$$

hence

$$W_{cr}(s)=\frac{1}{2T_{\mu c}s\left(T_{\mu c}s+1\right)}\cdot\frac{\left(T_{\mu c}s+1\right)\left(a_1 s^{1+\mu}+a_0 s^{\mu}+1\right)}{k_{conv}k_{cs}K}. \quad (13)$$

We obtain upon transforms

$$W_{cr}(s)=K_1 s s^{\mu_{co}-1}+K_2 s^{\mu_{co}-1}+K_3 p^{-1}, \quad (14)$$

where coefficients are

$$K_1=\frac{a_1}{2T_{\mu c}k_{conv}k_{cs}K},$$
$$K_2=\frac{a_0}{2T_{\mu c}k_{conv}k_{cs}K},$$
$$K_3=\frac{1}{2T_{\mu c}k_{conv}k_{cs}K}. \quad (15)$$

For the examined object, we obtained a D$^{\mu}$I$^{\gamma}$I controller (K_1=0.27, K_2=5.539, K_3=43.581); the diagram of current transient process is shown in Fig. 6 and corresponds exactly to the indicators for a modular optimum.

Configure the system with fractional orders of astatism $\mu=\mu_{co}$=0.3533 and μ=0.6. This will improve the

performance speed of control system thereby reducing overshooting.

$$W_{op.c}(s)=\frac{1}{aT_{\mu c}^{\mu}s^{\mu}\left(T_{\mu c}s+1\right)}=$$
$$=W_{cr}(s)\frac{k_{conv}}{\left(T_{\mu c}s+1\right)}\frac{K}{\left(a_0s^{1+\mu_{co}}+a_1s^{\mu_{co}}+1\right)}k_{cs}, \quad (16)$$

hence

$$W_{cr}(s)=\frac{1}{aT_{\mu c}^{\mu}s^{\mu}\left(T_{\mu c}s+1\right)}\cdot\frac{\left(T_{\mu c}s+1\right)\left(a_1s^{1+\mu_{\prec c}}+a_0s^{\mu_{\prec c}}+1\right)}{k_{conv}k_{cs}K}. \quad (17)$$

We obtain upon transforms

$$W_{cr}(s)=K_1ss^{\mu_{co}-\mu}+K_2s^{\mu_{co}-\mu}+K_3s^{-\mu}. \quad (18)$$

Therefore, the coefficients are:

$$K_1=\frac{a_1}{aT_{\mu c}^{\mu}k_{conv}k_{cs}K},$$

$$K_2=\frac{a_0}{aT_{\mu c}^{\mu}k_{conv}k_{cs}K},$$

$$K_3=\frac{1}{aT_{\mu c}^{\mu}k_{conv}k_{cs}K}, \quad (19)$$

where a configuration parameter

$$a\approx\frac{\mu}{4.683-5.897\mu+1.595\mu^2}$$

ensured the best ratio between performance and overshooting.

The results of simulating a current circuit with an astatism order of $\mu=\mu_{co}$ ($PI^{\gamma}D$ controller, K_1=0.218, K_2=4.465, K_3=35.135) and μ=0.6 ($D^{\mu}I^{\gamma}I^{\nu}$ controller, K_1=0.245, K_2=5.03, K_3=39.579) are also shown in Fig. 6.

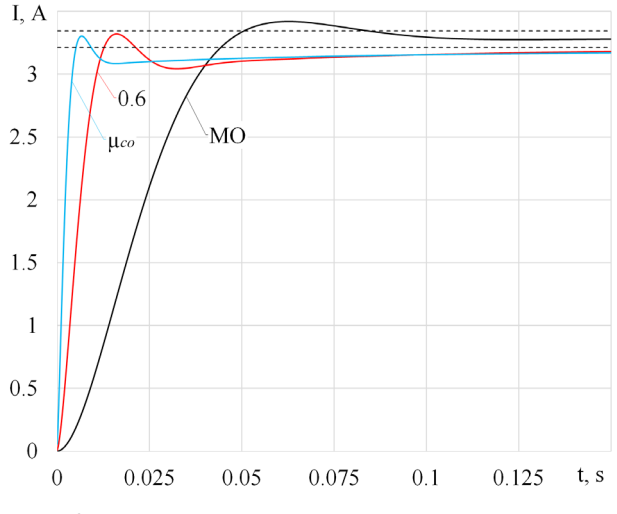

Fig. 6. Diagrams of transient processes set at a modular optimum and a fractional order of astatism $\mu=\mu_{co}$, μ=0.6

The disadvantage of the latter settings is that it takes long for current to approach the predefined value.

Of greatest interest is setting a fractional order of astatism 1+μ, μϵ(0; 1), at which not only static but also dynamic accuracy of the system improve.

To this end, we derive a transfer function of the controller from equation:

$$W_{op.c}(s)=\frac{1}{0T_{\mu c}^{\mu-1}s^{\mu-1}}\frac{bT_{\mu c}s+1}{bT_{\mu c}s}\frac{1}{\left(T_{\mu c}s+1\right)}=$$
$$=W_{cr}(s)\frac{k_{conv}}{T_{\mu c}s+1}\frac{K}{a_0s^{1+\mu_{co}}+a_1s^{\mu_{co}}+1}k_{cs}, \quad (20)$$

where values a and b are chosen approximately from the following ratios:

$$\begin{cases}(ba)\approx\exp(-10.27+7.831\mu),\\ b\approx7.336+0.792(ba)+3.83\ln(ba),\end{cases} \quad (21)$$

hence

$$W_{cr}(s)=\frac{1}{aT_{\mu c}^{\mu-1}s^{\mu-1}}\frac{bT_{\mu c}s+1}{bT_{\mu c}s}\frac{1}{\left(T_{\mu c}s+1\right)}\times$$
$$\times\frac{\left(T_{\mu c}s+1\right)\cdot\left(a_1s^{1+\mu_{co}}+a_0s^{\mu_{co}}+1\right)}{k_{conv}k_{cs}K}. \quad (22)$$

Following the transforms, we obtain a transfer function of the controller composed of six components:

$$W_{cr}(s)=K_0s^{-(\mu-1)}\begin{bmatrix}K_1s^2s^{\mu_{co}-1}+K_2ss^{\mu_{co}-1}+\\+K_3s^{\mu_{co}-1}+K_4s^{-1}+K_5\end{bmatrix}, \quad (23)$$

where

$$K_0=\frac{1}{aT_{\mu c}^{\mu-1}},$$

$$K_1=\frac{a_1}{k_{conv}k_{cs}K},$$

$$K_2=\frac{a_0bT_{\mu c}+a_1}{bT_{\mu c}k_{conv}k_{cs}K},$$

$$K_3=\frac{a_0}{bT_{\mu c}k_{conv}k_{cs}K},$$

$$K_4=\frac{1}{bT_{\mu c}k_{conv}k_{cs}K},$$

$$K_5=\frac{1}{k_{conv}k_{cs}K}. \quad (24)$$

For μ=1.5, we obtain K_0=37.04, K_1=0.0054, K_2=0.144, K_3=0.683, K_4=5.376, K_5=0.872, and at $\mu=1+\mu_{co}$ K_0=35.09, K_1=0.0054, K_2=0.167, K_3=1.158, K_4=9.11, K_5=0.872. The simulation results are shown in Fig. 7. It is evident that the performance improved while overshooting, compared with a modular optimum configuration, decreased by more than 2 times.

The transient processes, shown in Fig. 6, 7, were obtained without taking into consideration a power supply voltage limitation. However, the source of the experimental bench makes it possible to supply 24 volts only. As a result, the transient

characteristics do not match the estimated ones with the process quality indicators significantly worse (Fig. 8).

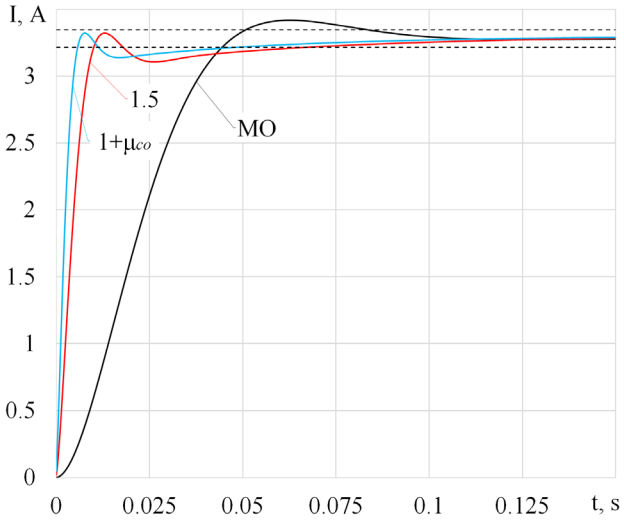

Fig. 7. Diagrams of transient processes set on a modular optimum and a fractional astatism of order $\mu=1+\mu_{co}$, $\mu=1.5$

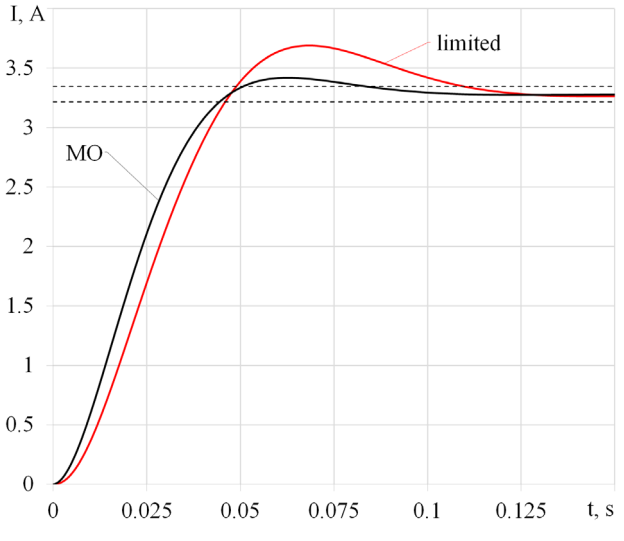

Fig. 8. Diagrams of transient processes with and without power voltage limitation

We shall change the structure of controllers and determine their parameters for ensuring optimal transient processes in terms of performance and overshooting.

6. Search for optimal parameters of controllers at a limited voltage of power source

To find the optimal coefficients, we used one of variants of the genetic algorithm in which a support function varies, based on which we assessed the fitness function of each individual [24]. We also selected the ranges of coefficients over which we searched for values: for a controller with the structure $D^{\mu}I^{\gamma}I$ $K_1\epsilon[1;20]$, $K_2\epsilon[1;80]$, $K_3\epsilon[1;60]$. Then, by crossbreeding and selection of individuals, we found the most suitable solution. For example, for $D^{\mu}I^{\gamma}I$-controller (Fig. 9), we obtained coefficients $K_1=1.746$, $K_2=40.75$, $K_3=12.428$ (instead of $K_1=0.27$, $K_2=5.539$, $K_3=43.581$, determined earlier); related diagrams are shown in Fig. 10.

One can see that the dynamic indicators for the system are better than in any of the cases in Fig. 8.

The selection of values for coefficients in control systems that are configured on a fractional order of astatism $\mu=0.6$ and $\mu=\mu_{co}$ was performed based on schematic diagrams of controllers from Fig. 11, *a, b,* respectively. The controller in Fig. 11, *a* was supplemented with a filter with a time constant $T_f=0.0006$ to suppress the noise from a differentiating component. Coefficients at $\mu=0.6$–$K_1=0.2$, $K_2=37.246$, $K_3=1.288$, at $\mu=\mu_{co}$–$K_1=0.0068$, $K_2=29.24$, $K_3=25.242$. Results from experimental study and simulation are shown in Fig. 12, *a* and Fig. 12, *b*.

Compared with a modular optimum, a noise level increases and the steady value is slightly less than the assigned value. The first harmonization time is $t_c=0.0344$ s, making these systems more responsive. However, the best properties of the transient process are demonstrated by variant $\mu=\mu_{co}$: both noise level and overshooting reduced. In addition, the controller's subroutine eliminates the need to compute signals from two fractional integrators of a different order.

By conducting a similar study for the system with orders of astatism of $\mu=1+\mu_{co}$ and $\mu=1.5$, we obtained regulators with structural diagrams, shown in Fig. 13, and respective transient processes (Fig. 14).

Coefficients of regulators at $T_f=0.0006$ s: for $\mu=1.5$–$K_0=0.393$, $K_1=0.118$, $K_2=29.31$, $K_3=66.22$, $K_4=170.54$, $K_5=1.969$; for $\mu=1+\mu_{co}$–$K_1=0.0193$, $K_2=16.63$, $K_3=44.19$, $K_4=26.52$, $K_5=4.452$. One can see that setting at $\mu=1.5$ has a somewhat protracted process in the region of ±2 % from the assigned value; in contrast to the model, there is no overshooting. When configuring at $\mu=1+\mu_{co}$, one almost immediately achieves the steady value over the time of first harmonization $t_c=0.0344$ without overshooting.

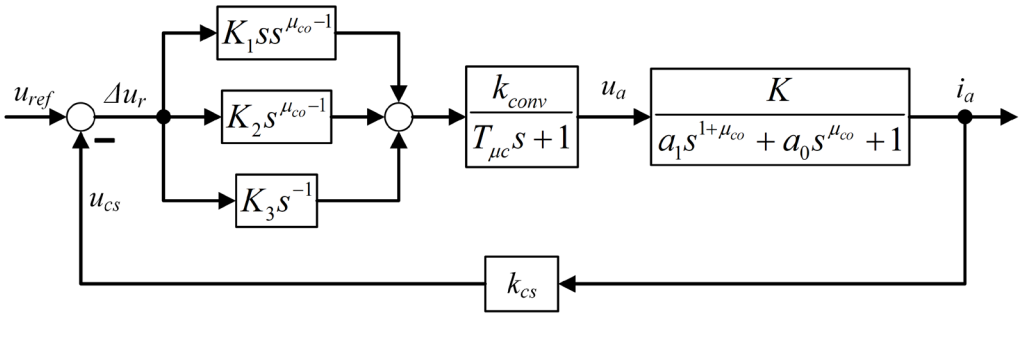

Fig. 9. Schematic diagram of the closed control system with a $D^{\mu}I^{\gamma}I$-controller

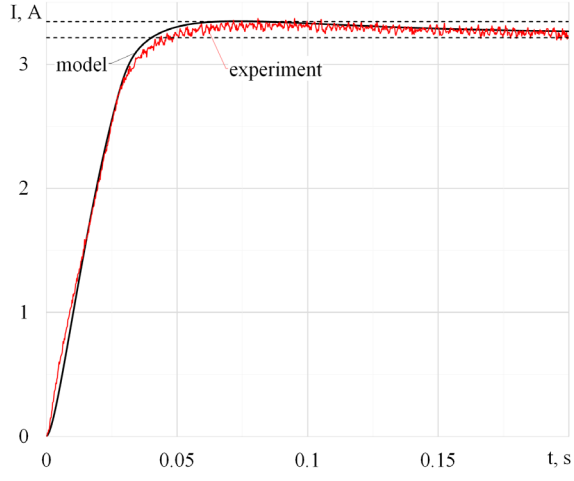

Fig. 10. Diagrams of transient processes with the optimized $D^{\mu}I^{\gamma}I$-controller

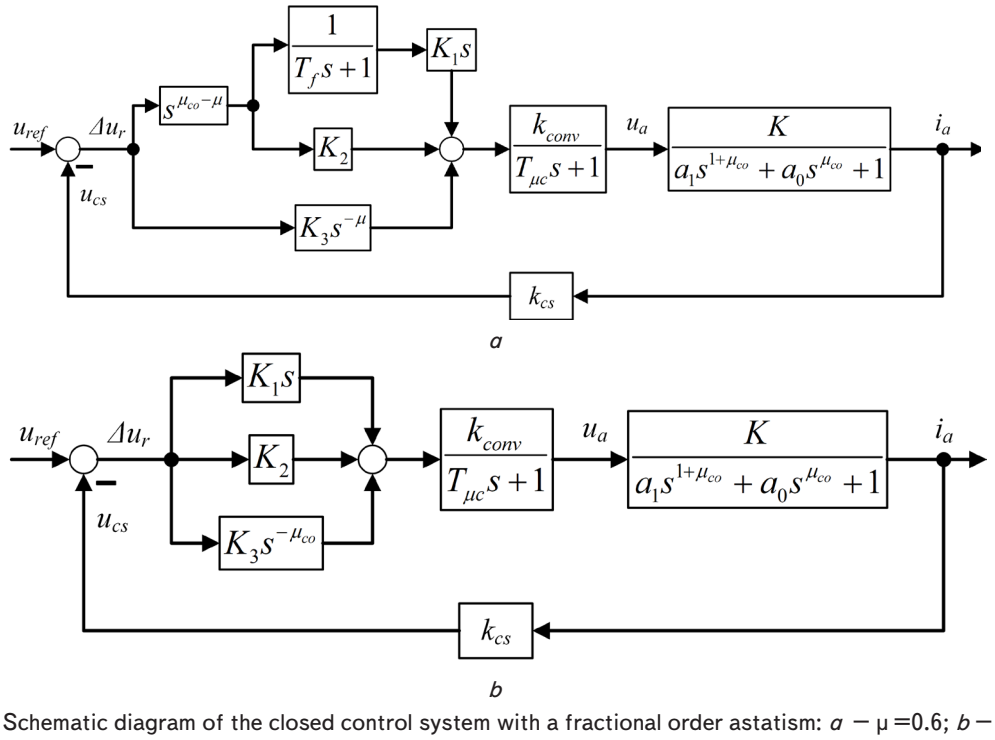

Fig. 11. Schematic diagram of the closed control system with a fractional order astatism: *a* – μ =0.6; *b* – μ =μ_{co}

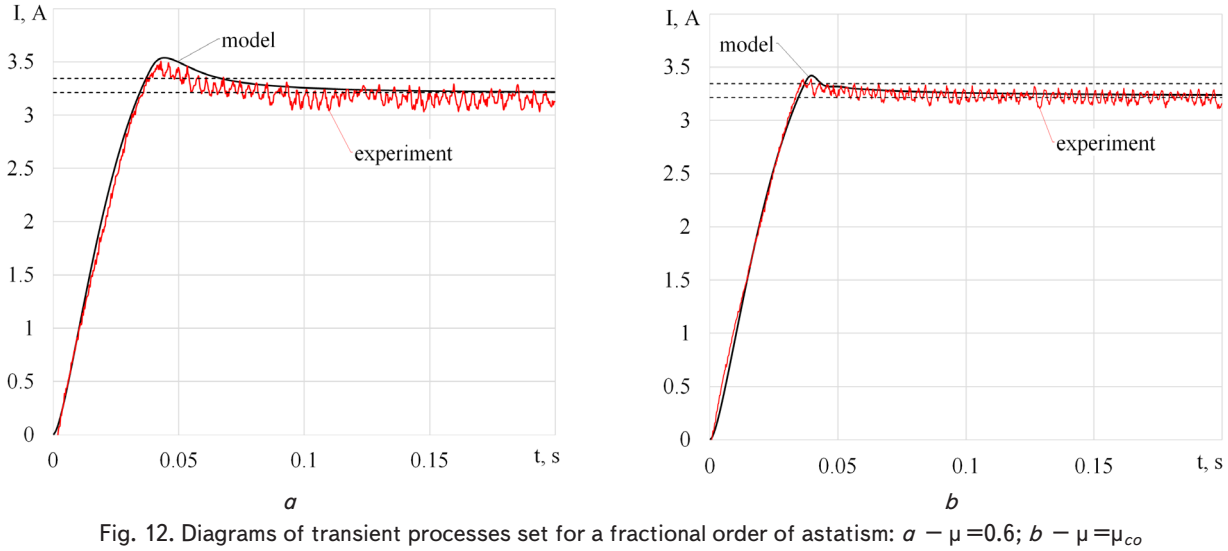

Fig. 12. Diagrams of transient processes set for a fractional order of astatism: *a* – μ =0.6; *b* – μ =μ_{co}

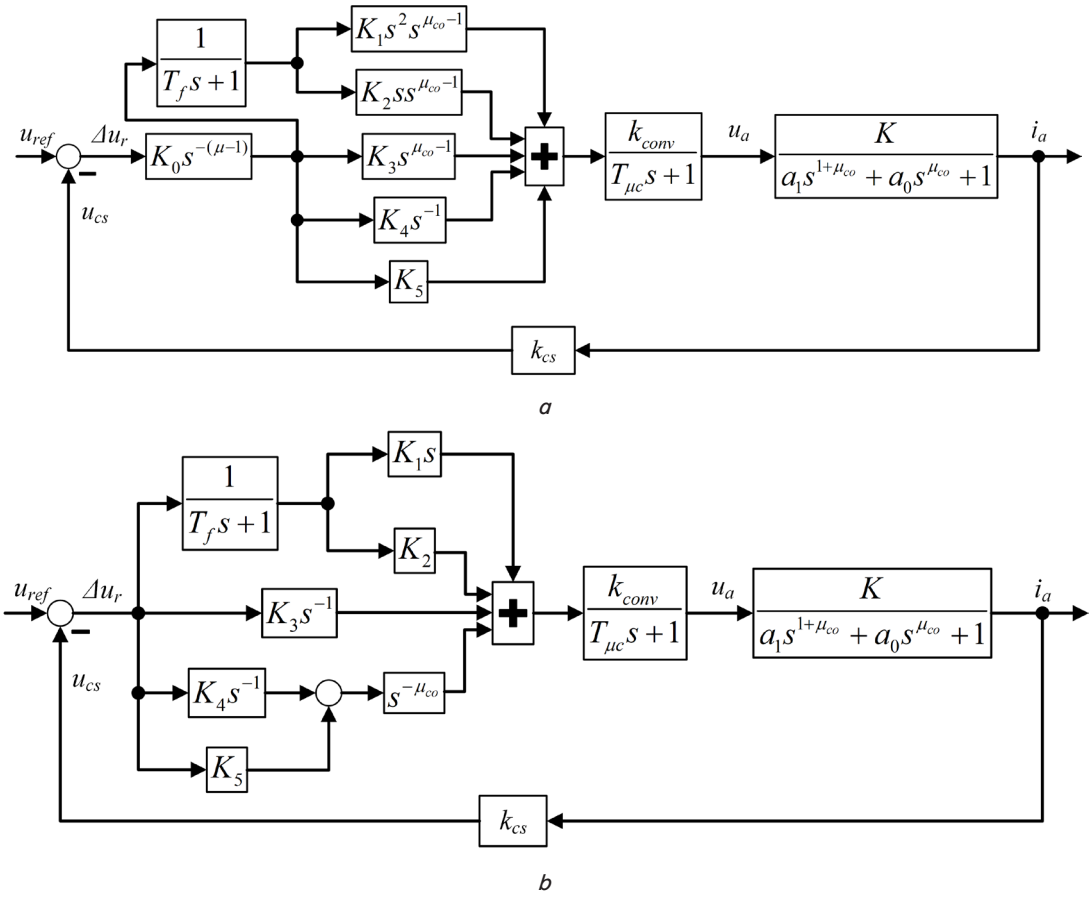

Fig. 13. Schematic diagram of the closed control system with a fractional order of astatism: *a* – μ =1.5; *b* – μ =1+μ_{co}

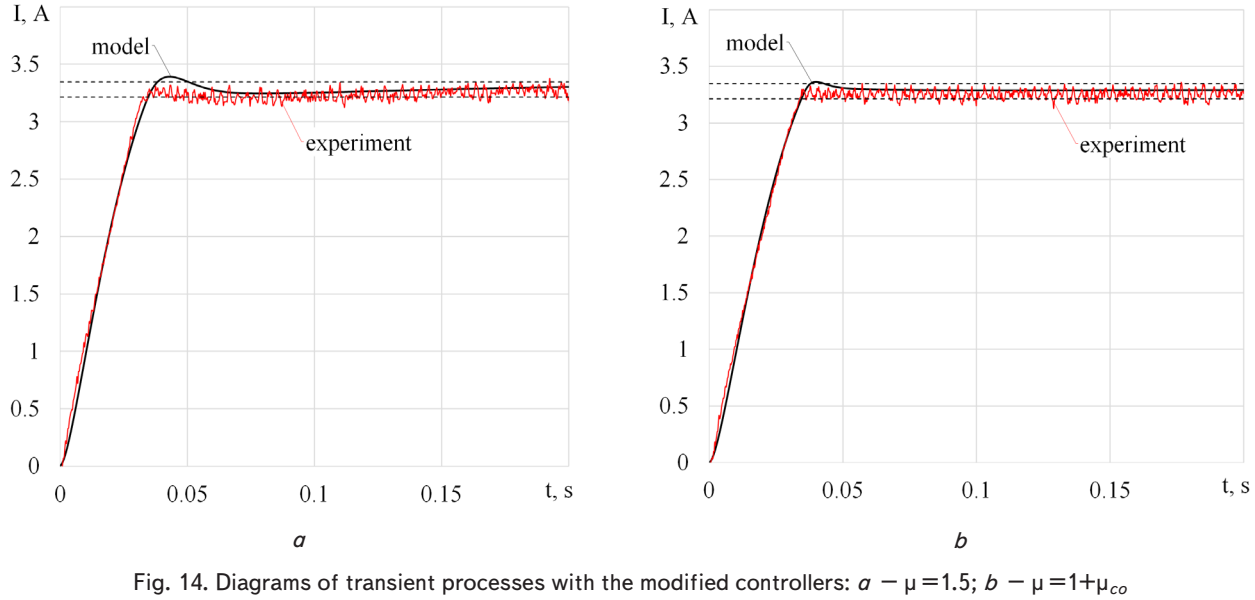

Fig. 14. Diagrams of transient processes with the modified controllers: *a* – μ =1.5; *b* – μ =1+μ_{co}

Such results were obtained at a relatively large current ($2I_n$) when there is a clearly pronounced nonlinearity due to the saturation of the magnetic system. What will happen if the motor operates in a linear region with a current less than the rated 1.6 A. For verification, without changing the structure of the controller configured for μ=1+μ_{co}, we performed simulation and experiments with the job signal reduced by half (Fig. 15, *a*). We also verified response from the system to step-wise changes in the job (Fig. 15, *b*).

In the course of simulation and experiments, qualitative indicators of the system remain unchanged and correspond to the desired settings. This is the crucial difference from the linearized system with a PI-controller (Fig. 3).

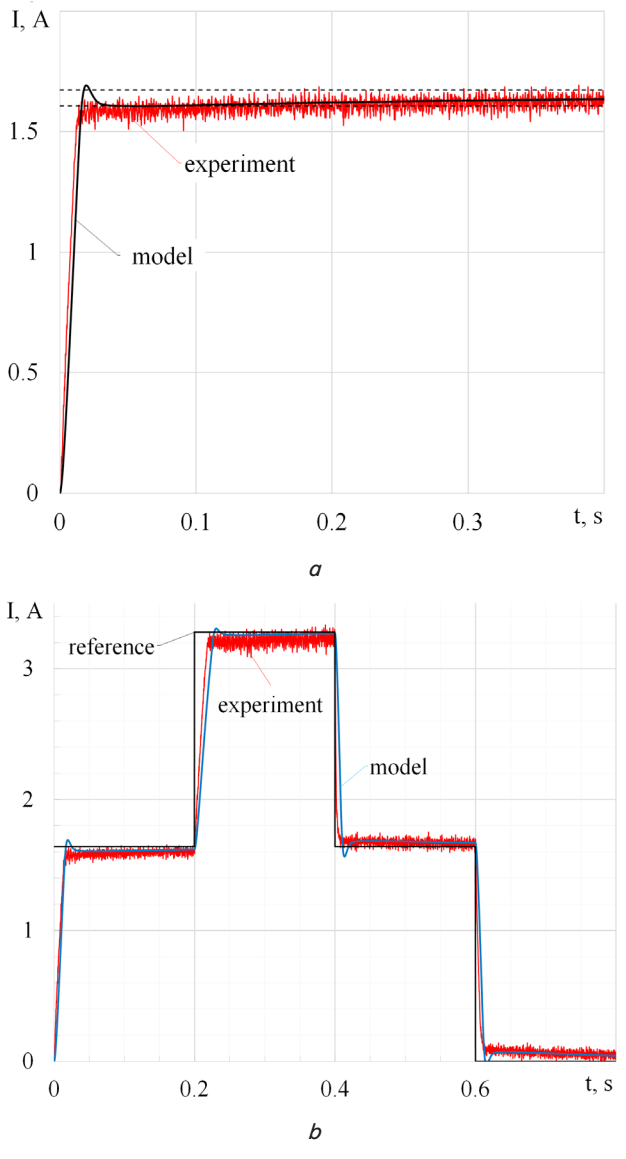

Fig. 15. Diagrams of transient processes with a controller for $\mu=1+\mu_{co}$: *a* – with a job signal of 1.6 A; *b* – at a step-wise change in the job signal

7. Discussion of results of synthesizing the controllers with a fractional order in the current circuit

We have examined various settings of the current closed circuit with an integer and fractional order of astatism for the motor with series excitation. We compared results from simulation and experimental study at settings for a modular optimum and with fractional orders of astatism μ_{co}, 0.6, $1+\mu_{co}$, 1.5 (Fig. 10, 12, 14, 15). The findings suggest, first, that the chosen mathematical model of control object is in good agreement with the experiment, especially when current is 2 times larger than rated. Even in the linear region (up to the level of the rated current), the differences are relatively small – there a slight overshooting in the system model, not observed during experiments (Fig. 15, *a*).

Second, each setting has its advantages and disadvantages:

– at the $D^{\mu}I^{\gamma}I$ structure of the controller (Fig. 10), the transient process has almost no overshooting – less than 2 %, but it is prolonged in time in the region of ±2 % of the assigned value;

– under settings for a fractional order of astatism 0.6 and μ_{co}, the presence of a differential link in the controller intensified disturbances, causing instability and enhanced oscillation at certain values of coefficients. That necessitated limitations on these coefficients for the genetic algorithm. The best results for controllers under these settings are shown in Fig. 12. The first harmonization is less by 0.006 s than that in the previous case. However, during motor operation, there are disturbances observed, overshooting exceeds 2 %, under a steady mode, a static error appears, albeit less than 2 %;

– when configured for a fractional order of astatism of 1.5, the structure of the controller becomes more complicated (Fig. 13, *a*). However, that makes it possible to compensate for those shortcomings that were obtained for the case of a fractional astatism of 0.6 and μ_{co}. The overshooting is small, the time of first harmonization is 0.0344 s, but there is a prolongation of the transient process in the region of ±2 % of the preset value (Fig. 14, *a*);

– when configured for a fractional order of astatism $1+\mu_{co}$, the transient process outperforms all previous settings (Fig. 14, *b*), the only disadvantage includes somewhat increased current pulsations compared with the $D^{\mu}I^{\gamma}I$ controller.

Thus, it can be argued that among the options considered the use of a controller set for a fractional order of astatism $1+\mu_{co}$ yields the best results in a closed current circuit of the motor with series excitation. An experiment with job signals 0→1.64 A→3.28 A→1.64 A→0 demonstrates that a given setting is also applicable over the entire range of current control.

The results obtained can be used in the future to build control systems of valve-jet engines, asynchronous electric drives with vector control.

8. Conclusions

1. An experimental study of DCMSE at a current of $2I_n$ and subsequent processing of data have shown that the motor armature circuit is most accurately described by a fractional-differential equation of order $1+\mu_{co}$ ($\mu_{co}\approx0.35$) and, accordingly, transfer function $W_{co3}=\dfrac{K}{a_1 s^{1+\mu}+a_0 s^{\mu}+1}$.

2. We have investigated a closed-loop system set for modular optimum, for an optimum with orders of astatism 0.6, μ_{co}, 1.5, $1+\mu_{co}$. The respective structural schemes and parameters for controllers have been determined. The best dynamic and static indicators characterize the system with an order of $1+\mu_{co}$, including under conditions for a power supply voltage limitation. To ensure such a configuration, a controller is required with the structure shown in Fig. 14, *b*, whose parameters can be found using genetic algorithms. When such a controller is discretely implemented in a loop, there is a single calculation of the fractional integral, which reduces the requirements to computational power and to memory volume in a microprocessor.

3. It is shown that such a closed system retains the optimal properties at different levels of jobs from 0 to $2I_n$, which characterizes it as a self-similar one. Therefore, it becomes feasible to analyze and synthesize using classical methods of the theory of automatic control for linear systems.

References

1. Vasil'ev V. V., Simak L. A. Drobnoe ischislenie i approksimacionnye metody v modelirovanii dinamicheskih sistem. Kyiv, 2008. 256 p.
2. Uchaykin V. V. Metod drobnyh proizvodnyh. Ul'yanovsk: Izdatel'stvo «Artishok», 2008. 512 p.
3. Uchaikin V. V. Fractional Derivatives for Physicists and Engineers. Springer, 2013. 385 p. doi: https://doi.org/10.1007/978-3-642-33911-0
4. Tarasov V. E. Fractional Dynamics. Applications of Fractional Calculus to Dynamics of Particles, Fields and Media. Heidelberg, 2010. 505 p.
5. The Fractional Calculus: Theory and Applications of Differentiation and Integration to Arbitrary Order / K. B. Oldham, J. Spanier (Eds.). Elsevier, 1974. 322 p. doi: https://doi.org/10.1016/s0076-5392(09)x6012-1
6. Hilfer R. Applications of Fractional Calculus in Physics. World Scientific, 2000. 472 p. doi: https://doi.org/10.1142/3779
7. Anomalous relaxation in dielectrics / Novikov V. V., Wojciechowski K. W., Komkova O. A., Thiel T. // Equations with fractional derivatives. Materials Science-Poland. 2005. Vol. 23, Issue 4. P. 977–984.
8. Influence of magnetic circuit saturation and skin effects on the adjustable induction motor characteristics / Petrushin V., Bendahmane B., Yahiaoui B., Yakimets A. // International Journal of Hydrogen Energy. 2017. Vol. 42, Issue 48. P. 29006–29013. doi: https://doi.org/10.1016/j.ijhydene.2017.07.221
9. Doradla S. R., Sen P. C. Time ratio control (TRC) scheme for a DC series motor Part II: Commutation circuit analysis // Canadian Electrical Engineering Journal. 1978. Vol. 3, Issue 2. P. 44–48. doi: https://doi.org/10.1109/ceej.1978.6591134
10. Sen P. C., Doradla S. R. Time ratio control (TRC) scheme for a DC series motor Part I: Performance // Canadian Electrical Engineering Journal. 1978. Vol. 3, Issue 2. P. 39–43. doi: https://doi.org/10.1109/ceej.1978.6591133
11. Alexandridis A. T., Konstantopoulos G. C. Modified PI speed controllers for series-excited dc motors fed by dc/dc boost converters // Control Engineering Practice. 2014. Vol. 23. P. 14–21. doi: https://doi.org/10.1016/j.conengprac.2013.10.009
12. Rengifo Rodas C. F., Castro Casas N., Bravo Montenegro D. A. A performance comparison of nonlinear and linear control for a DC series motor // Ciencia en Desarrollo. 2017. Vol. 8, Issue 1. P. 41–50. doi: https://doi.org/10.19053/01217488.v8.n1.2017.5455
13. Robust Takagi-Sugeno fuzzy speed regulator for DC series motors / Farooq U., Gu J., Asad M. U., Abbas G. // 2014 12th International Conference on Frontiers of Information Technology. 2014. doi: https://doi.org/10.1109/fit.2014.24
14. Valluru S. K., Singh M., Kumar N. Implementation of NARMA-L2 Neuro controller for speed regulation of series connected DC motor // 2012 IEEE 5th India International Conference on Power Electronics (IICPE). 2012. doi: https://doi.org/10.1109/iicpe.2012.6450518
15. Petrás I. Fractional – order feedback control of a dc motor // Journal of Electrical Engineering. 2009. Vol. 60, Issue 3. P. 117–128. URL: https://pdfs.semanticscholar.org/a033/af254d22cc8bfc979341bd8af6e3c76a07a6.pdf
16. Copot C., Muresan C. I., De Keyser R. Speed and position control of a DC motor using fractional order PI-PD control // 3rd International Conference on Fractional Signals and Systems. Ghent, 2013. URL: https://core.ac.uk/download/pdf/55870474.pdf
17. Heidarpoor S., Tabatabaei M., Khodadadi H. Speed control of a DC motor using a fractional order sliding mode controller // 2017 IEEE International Conference on Environment and Electrical Engineering and 2017 IEEE Industrial and Commercial Power Systems Europe (EEEIC / I&CPS Europe). 2017. doi: https://doi.org/10.1109/eeeic.2017.7977822
18. Tajbakhsh H., Balochian S. Robust Fractional Order PID Control of a DC Motor with Parameter Uncertainty Structure // International Journal of Innovative Science, Engineering & Technology. 2014. Vol. 1, Issue 6. P. 223–229. URL: http://www.ijiset.com/v1s6/IJISET_V1_I6_37.pdf
19. Petras I. Fractional Derivatives, Fractional Integrals, and Fractional Differential Equations in Matlab // Engineering Education and Research Using MATLAB. 2011. doi: https://doi.org/10.5772/19412
20. Das S., Pan I. Fractional Order Signal Processing // SpringerBriefs in Applied Sciences and Technology. Springer, 2012. doi: https://doi.org/10.1007/978-3-642-23117-9
21. Marushchak Y. Y., Kopchak B. L. Synthesis fractional order controllers for electromechanical systems // Elektrotekhnichni ta kompiuterni systemy. 2017. Issue 25. P. 26–33. URL: http://nbuv.gov.ua/UJRN/etks_2017_25_6
22. Busher V., Aldairi A. Synthesis and technical realization of control systems with discrete fractional integral-differentiating controllers // Eastern-European Journal of Enterprise Technologies. 2018. Vol. 4, Issue 2 (94). P. 63–71. doi: https://doi.org/10.15587/1729-4061.2018.139892
23. Kuvshinov A. A. Teoriya elektroprivoda. Ch. 1. Orenburg, 2009. 197 p.
24. Rutkovskaya D., Pilin'skiy M., Rutkovskiy L. Neyronnye seti, geneticheskie algoritmy i nechetkie sistemy. Moscow, 2006. 452 p.